

Is the new CDF M_W measurement consistent with the two higgs doublet model?

H. ABOUABID^{1*}, A. ARHRIB^{1†}, R. BENBRIK^{2‡}, M. KRAB^{3§}, M. OUCHEMHOU^{2¶}

¹ Abdelmalek Essaadi University, Faculty of Sciences and Techniques, Tangier, Morocco.

² Laboratory of Fundamental and Applied Physics, Faculté Polydisciplinaire de Safi, Sidi Bouzid, BP 4162, Safi, Morocco.

³ Research Laboratory in Physics and Engineering Sciences, Modern and Applied Physics Team, Polidisciplinary Faculty, Beni Mellal, 23000, Morocco.

Abstract

Motivated by the new CDF measurement of the W boson mass reported recently which clearly illustrates a large deviation compared to the Standard Model (SM) prediction. In the present paper, we study the Two-Higgs Doublet Model (2HDM) contributions to M_W and its phenomenological implications in the case where the heavy CP-even H is identified as the observed Higgs boson with a mass of 125 GeV. Taking into account theoretical and all the available experimental constraints as well as the new CDF measurement, we demonstrate that the 2HDM parameter space can provide a large correction which predicts the W mass close to the new CDF M_W measurement. It is found that $M_{H^\pm} = M_A$ is excluded and the splitting of the charged Higgs boson with all other states is positive. We also discuss the consequences on the effective mixing angle $\sin^2 \theta_{\text{eff}}$ as well as the phenomenological implications on the charged Higgs and CP-odd Higgs boson decays in 2HDM type I and type X.

*hamza.abouabid@gmail.com

†aarhrib@gmail.com

‡r.benbrik@uca.ma

§mohamed.krab@usms.ac.ma

¶ouchemhou2@gmail.com

1 Introduction

ElectroWeak Precision Observables (EWPOs) such as W boson mass, the effective mixing angle $\sin^2 \theta_{\text{eff}}$ and the Z boson width etc, can be used to test the validity Standard Model (SM) and to reveal the presence of new physics.

After a decade of work, using the data set collected at 8.8 fb^{-1} luminosity and 1.96 TeV center-of-mass energy at the Tevatron, the CDF collaboration discovered that the W boson has a mass of [1, 2]:

$$M_W^{\text{CDF}} = 80.4435 \pm 0.0094 \text{ GeV}. \quad (1)$$

The precision with which this measurement was carried out, 0.01%, exceeds all previous measurements combined. In addition, the new value agrees with many previous W mass measurements, but there are also some disagreements [3]. Therefore, future measurements will be needed to further shed light on the outcome. The above measurement should be compared to the SM prediction [3, 4],

$$M_W^{\text{SM}} = 80.357 \pm 0.006 \text{ GeV}. \quad (2)$$

Note that the above value is based on complex SM radiative corrections that closely relate the mass of the W to the measurements of the masses of the top quark and the Higgs boson. It is clear that M_W^{CDF} presents a deviation from M_W^{SM} with a significance of 7.0σ .

In the past, during the LEP era, it was well known that the global fit of the SM to LEP and SLC data has been used to predict the existence of heavy top quark and relatively light Higgs boson well before their discovery at Tevatron and LHC respectively. Although the CDF measurement needs to be confirmed shortly, it is quite likely that the difference between the experimental value and the expected SM value is due to a non-decoupled new particle or a new interaction. If it is the case, there is a chance that these new phenomena will show up in future experiments.

Moreover, it is well known that the discrepancy of M_W^{CDF} from the SM prediction can be parameterized in terms of the oblique parameters, S , T and U [5, 6] which are a combination of gauge bosons self energies. All new particles, if not too heavy and interact with the photon, W and Z bosons, will contribute to S , T and U and can therefore reduce the tension between M_W^{CDF} and M_W^{SM} .

In the present paper, we will discuss the implications of the new CDF measurement on the Two-Higgs Doublet Model (2HDM) which predicts in its spectrum 2 CP-even, h and H (with $M_h < M_H$), one CP-odd A and a pair of charged Higgs H^\pm . Recently, there have been several studies addressing a similar issue within: the 2HDM [7–20], triplet extension [21–24] and also other SM extensions [25–49]. In this study, we identify the observed SM Higgs with H whose properties are consistent with the LHC measurements and assume that the second CP-even Higgs is lighter than 125 GeV. We will explain how the 2HDM can solve the tension between CDF measurement and the SM prediction and give some phenomenological implications on charged Higgs and CP-odd Higgs boson decays both in 2HDM type I and type X.

The paper is organized as follows, in the second section we briefly introduce the set-up of the 2HDM and give the S , T and U formalism for the computation of $M_W^{2\text{HDM}}$ and $\sin^2 \theta_{\text{eff}}^{2\text{HDM}}$. In the third section, we present the details of our scan as well as the theoretical and experimental constraints used to constrain the parameter space. We then present our main result and explain how the 2HDM spectrum can predict the W mass that is close to the new CDF measurement. In addition, we give phenomenological implications for the charged Higgs and CP-odd boson decays within the allowed parameter space. We conclude in section four.

2 M_W in the 2HDM

The 2HDM framework is one of the simplest extensions of the SM Higgs sector. It contains two Higgs doublet fields, ϕ_1 and ϕ_2 , that can interact with fermions and gauge bosons to generate their masses.

The most general scalar potential which is invariant under $SU_L(2) \times U_Y(1)$ and CP-conserving can be written as

$$\begin{aligned}
 V(\phi_1, \phi_2) &= m_{11}^2(\phi_1^\dagger\phi_1) + m_{22}^2(\phi_2^\dagger\phi_2) - [m_{12}^2(\phi_1^\dagger\phi_2) + \text{h.c.}] \\
 &+ \frac{1}{2}\lambda_1(\phi_1^\dagger\phi_1)^2 + \frac{1}{2}\lambda_2(\phi_2^\dagger\phi_2)^2 + \lambda_3(\phi_1^\dagger\phi_1)(\phi_2^\dagger\phi_2) \\
 &+ \lambda_4(\phi_1^\dagger\phi_2)(\phi_2^\dagger\phi_1) + \frac{1}{2}[\lambda_5(\phi_1^\dagger\phi_2)^2 + \text{h.c.}], \tag{1}
 \end{aligned}$$

where $\lambda_{1,2,3,4,5}$ as well as m_{11}^2 and m_{22}^2 are chosen to be real. If both Higgs fields interact with all SM fermions, like in the SM, we end up with Flavour Changing Neutral Currents (FCNCs) at the tree-level in the Yukawa sector. In order to avoid such FCNCs, a discrete Z_2 symmetry is introduced to prevent large tree-level FCNCs [50, 51]. Such a discrete symmetry is imposed both on the Yukawa sector as well as the scalar potential where we allow for a soft violation of Z_2 by $m_{12}^2(\phi_1^\dagger\phi_2)$ term. Moreover, under the Z_2 symmetry, there are four possible types of Yukawa sector: type I, type II, type X (or lepton-specific) and type Y (or flipped). Here, in this work, we shall focus on type I and X models. In the 2HDM type-I, ϕ_2 doublet couples to all the SM fermions exactly like in the SM while in the 2HDM type-X all the quarks couple to ϕ_2 and the charged leptons couple to ϕ_1 .

Using the two minimization conditions, m_{11}^2 and m_{22}^2 can be expressed as functions of other parameters. The combination of v_1 and v_2 is fixed from the electroweak scale: $v_1^2 + v_2^2 = v^2 \simeq (246 \text{ GeV})^2$. We thus end up with 7 independent parameters, namely $\lambda_{1,2,3,4,5}$, m_{12}^2 and $\tan\beta$. Alternatively, the set M_h , M_H , M_A , M_{H^\pm} , $\sin(\beta - \alpha)$, $\tan\beta$ and m_{12}^2 can be chosen instead. The angle α is the mixing angle between the two CP-even scalars h and H , while β is defined as the ratio of the vevs, $\tan\beta = v_2/v_1$.

The 2HDM contribution to the EWPOs can be described by the oblique parameters formalism, which is a good one for new physics. A convenient parametrization of such formalism is given by the well known parameters S , T and U [5, 6]. In the 2HDM, the ρ parameter, which is the ratio of neutral and charged current at small momentum transfer, is related to the oblique parameter T . Such a contribution is controlled by the so-called custodial symmetry to preserve the tree-level value of ρ parameter, $\rho = M_W^2/(c_W^2 M_Z^2) \approx 1$, which is in good agreement with experiments. As discussed in the literature, in the SM the custodial symmetry is broken both by the Hypercharge as well as by the different sizes of the Yukawas, while in the 2HDM the custodial symmetry can be restored in the scalar sector so long the Higgs states are degenerate in mass.

In general, the contribution of 2HDM to W boson mass can be expressed in terms of the parameters S , T and U [6], i.e.

$$\Delta M_W^2 = \frac{\alpha_0 c_W^2 M_Z^2}{c_W^2 - s_W^2} \left[-\frac{1}{2}S + c_W^2 T + \frac{c_W^2 - s_W^2}{4s_W^2} U \right], \tag{2}$$

where $\Delta M_W^2 = (M_W^{2\text{HDM}})^2 - (M_W^{\text{SM}})^2$, M_Z is the Z boson mass, $c_W = M_W^{\text{SM}}/M_Z$ and s_W are respectively cosine and sine of the weak mixing angle ($s_W^2 = 1 - c_W^2$) and α_0 is the fine structure constant at the Thomson limit.

We also study the effects of the 2HDM spectrum on the effective weak mixing angle, $\sin^2 \theta_{\text{eff}}$. This is computed using the following relation [6]:

$$\Delta \sin^2 \theta_{\text{eff}} = \frac{\alpha_0}{c_W^2 - s_W^2} \left[\frac{1}{4} S - s_W^2 c_W^2 T \right]. \quad (3)$$

Where $\Delta \sin^2 \theta_{\text{eff}}$ is the difference between the 2HDM and the SM value. Note that in both Eq. (2) and Eq. (3), the dominant correction to the W boson mass and $\sin^2 \theta_{\text{eff}}$ comes from T ($\equiv \delta\rho/\alpha_0$) parameter, which is sensitive to the mass splitting of 2HDM scalar particles. The size of T parameter could be viewed as the amount of violation of the Custodial symmetry by the 2HDM spectrum. The SM values used in our calculation are given in Ref. [3]. Analytic expressions for S , T and U parameters in the 2HDM are given in [52].

3 Results and discussions

To study the implication of the new CDF measurement on the 2HDM, we consider the 2HDM type I⁶ and perform a systematic scan over its parameter space. The scan is done using the public program 2HDMC-1.8.0 [52]. We assume that the CP-even Higgs boson H is the observed SM-like Higgs with $M_H = 125.09$ GeV [53] whose properties are consistent with the LHC measurements. In addition, we suppose that the light CP-even h is lighter than 125 GeV and check that it is consistent with the previous negative LEP and LHC searches. We randomly sample the remaining model parameters within the following ranges:

$$\begin{aligned} M_h &= 15 - 120 \text{ GeV}; & M_A &= 15 - 700 \text{ GeV}; \\ M_{H^\pm} &= 80 - 700 \text{ GeV}; & \sin(\beta - \alpha) &= -0.5 - 0.5; \\ \tan \beta &= 2 - 25; & m_{12}^2 &= 0 - M_h^2 \sin \beta \cos \beta. \end{aligned} \quad (4)$$

During the scan, the following theoretical and experimental constraints are fulfilled

- Unitarity, perturbativity and vacuum stability are imposed via 2HDMC.
- Exclusion bounds at 95% Confidence Level (CL) from additional Higgs bosons are enforced via HiggsBounds-5.9.0 [55].
- Compliance with SM-like Higgs state measurements are enforced via HiggsSignals-2.6.0 [56].
- Constraints from flavor physics are enforced using the result given in Ref. [54]. Related observables are calculated using the program SuperIso v4.1 [57].
- Compatibility with the Z width measurement from LEP, $\Gamma_Z = 2.4952 \pm 0.0023$ GeV [58]. The partial width $\Gamma(Z \rightarrow hA)$, when is kinematically open, was chosen to satisfy the 2σ experimental uncertainty of the measurement.

Once we get the allowed parameter space that satisfies all the above theoretical and experimental constraints, we then apply the following $\chi_{M_W^{\text{CDF}}}^2$ test where we take only points that are within 2σ of the new CDF measurement.

⁶The 2HDM contribution to ΔM_W is expected to be the same in all Yukawa types at the one-loop level. The main difference comes from LHC constraints on Higgs physics.

$$\chi_{M_W^{\text{CDF}}}^2 = \frac{(M_W^{2\text{HDM}} - M_W^{\text{CDF}})^2}{(\Delta M_W^{\text{CDF}})^2}, \quad (5)$$

where $\Delta M_W^{\text{CDF}} = 0.0094$ GeV is the uncertainty of the new CDF measurement (see Eq. 1).

In Figure 1 (left panel), we present the 2HDM prediction for the W boson mass in the allowed parameter as a function of T , where the color map shows the possible size of S . The light orange band shows the new CDF result for M_W within the 1σ uncertainty. We also depict via light black region the SM prediction at the 1σ level. As expected from Eq. (2), the dominant contribution arises from the T parameter which is almost a linear relation. M_W receives a negative correction from S as indicated by the color code. The dependence of U to M_W is found to be negligible compared to T . It is obvious from Eq. (2) that negative range of the S parameter and positive values of T and U are indeed favored by the new CDF measurement for M_W . Therefore, close to the alignment limit $\cos(\beta - \alpha) \approx 1$, the degenerate case $M_A = M_{H^\pm}$ of the 2HDM is excluded by this new measurement because it would make T vanish. We note that the allowed range for S and T parameters is consistent with the recent results found in the literature [7, 26, 29, 59].

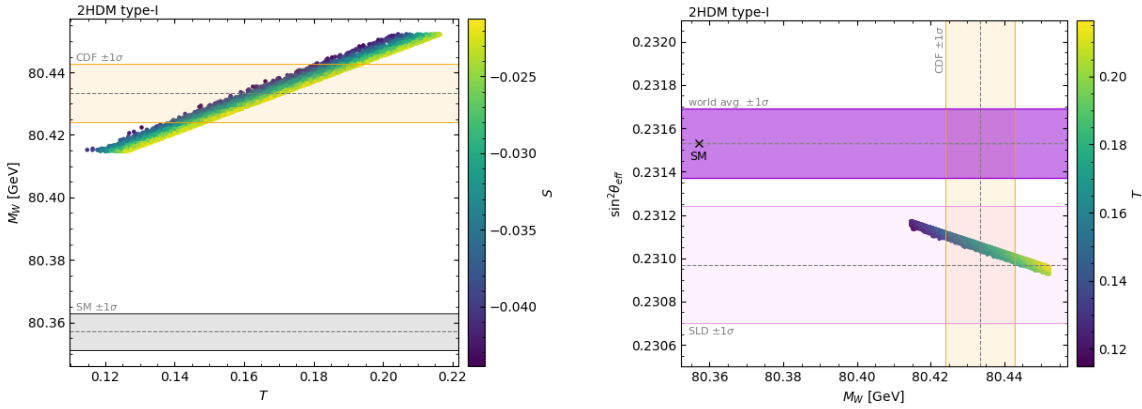


Figure 1: Left: The 2HDM prediction for the W boson mass as a function of T , with the color bar showing the size of S . The light orange band indicates the new CDF measurement and the associated 1σ uncertainty. The SM prediction for M_W is given by the light black region within $\pm 1\sigma$. Right: The 2HDM prediction for M_W and $\sin^2 \theta_{\text{eff}}$, with the color bar refers to T . The light orange band indicates the new CDF measurement and the associated 1σ uncertainty. The light and dark violet regions represent the SLD and world average results for $\sin^2 \theta_{\text{eff}}$ within the 1σ level, respectively. The SM prediction for M_W and $\sin^2 \theta_{\text{eff}}$ is given by the black cross.

Another important precision observable is the effective weak mixing angle, $\sin^2 \theta_{\text{eff}}$. The 2HDM prediction for M_W and $\sin^2 \theta_{\text{eff}}$ for the allowed points is depicted in the right panel of Figure 1. The light violet band indicates the SLD $\sin^2 \theta_{\text{eff}}$ measurement within the 1σ uncertainty [58]. We also show via the dark violet region the world average value for $\sin^2 \theta_{\text{eff}}$ at 1σ level (for the purpose of comparison) [58]. It can be seen clearly that M_W within the 2σ level is in good compliance with the SLD measurement which is not the case for the world average value.

As a first implication, we investigate the impact of the new CDF measurement on the spectrum of the 2HDM with inverted hierarchy. In the 2HDM with normal hierarchy: $m_h = 125$ GeV and $m_H > m_h$, it was shown recently in literature that both $M_{H^\pm} > M_H, M_A$ and $M_{H^\pm} < M_H, M_A$ are favored by the new CDF measurement for M_W , whereas the case where $M_{H^\pm} \sim M_H \sim M_A$ is

disfavored in the alignment limit of the 2HDM [11, 16].

In the 2HDM with inverted hierarchy, we illustrate in Figure 2 the splitting $M_{H^\pm} - M_A$ as a function of $M_{H^\pm} - M_h$ (left panel) and as a function of $M_{H^\pm} - M_H$ (right panel) with ΔM_W color coded and represented in the vertical panel. It is clear that the CDF M_W measurement force M_{H^\pm} to be always heavier than the neutral Higgses. The cases $M_{H^\pm} < M_h, M_H, M_A$ are excluded by the fact that it produces a negative or small T and therefore can not account for the new CDF measurement. Another outcome of the scan is that the new CDF M_W measurement push the charged Higgs mass to be larger than 161 GeV. For completeness, we show in Figure A1 of Appendix A the full scan for M_W as a function of S (left plot) and as a function of T (right plot). The green points are the one that reproduce the new CDF measurement while the blue points does not give the correct M_W mass. Similarly, we illustrate in Figure A2 of Appendix A the full scan for $M_{H^\pm} - M_A$ as a function of $M_{H^\pm} - M_h$ (left plot) and $M_{H^\pm} - M_A$ as a function of $M_{H^\pm} - M_H$ (right plot). Only the green band reproduce the new CDF measurement. It is clear from the plots that the new CDF measurement push the charged Higgs mass to be larger than 161 GeV.

The results shown in the previous plots are for 2HDM type I. For 2HDM type X, we obtain similar plots. The reason is that $\Delta M_W^{2\text{HDM}}$ depend only on S , T and U which are a combination of gauge boson self energies that contains the contribution of the additional Higgs bosons. The interaction of the gauge bosons to the Higgs boson does not depend on the Yukawa type. The only difference between type I and type X would come from the LHC constraints. Such constraints depend on the production cross section of the Higgs and its branching fractions which are sensitive to the Yukawa type. Note also that the combination of EWPOs as well as the theoretical constraints set a limit on the masses of the heavy states H^\pm and A^0 to be less than about 600 GeV.

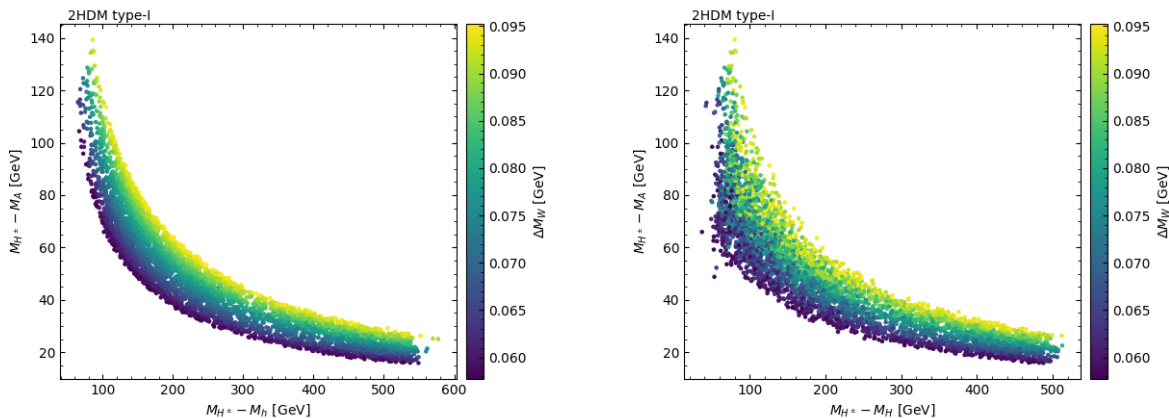


Figure 2: Points from the scan in the $(M_{H^\pm} - M_h, M_{H^\pm} - M_A)$ plane (left) and $(M_{H^\pm} - M_H, M_{H^\pm} - M_A)$ plane (right) planes in 2HDM type I. The color code indicates the shift from the SM prediction for M_W .

We move now to discuss phenomenological consequences on the charged Higgs, CP-odd Higgs and the light CP-even Higgs decays in 2HDM type I and type X. In the upper left-upper panel of Figure 3, we depict the branching ratios of H^\pm as a function of M_{H^\pm} . As one can see, the dominant decay of the charged Higgs are the bosonic channels: $H^\pm \rightarrow W^\pm h$ and $H^\pm \rightarrow W^\pm A$. For charged Higgs mass less than 200 GeV, both channels $H^\pm \rightarrow W^\pm h$ and $H^\pm \rightarrow W^\pm A$ compete. The decay $H^\pm \rightarrow W^\pm h$ enjoy more phase space because $M_h < 125$ GeV, while the decay $H^\pm \rightarrow W^\pm A$ is open only for a small portion of the phase space when $M_{H^\pm} - M_A > 80$ GeV. In fact, when $H^\pm \rightarrow W^\pm A$

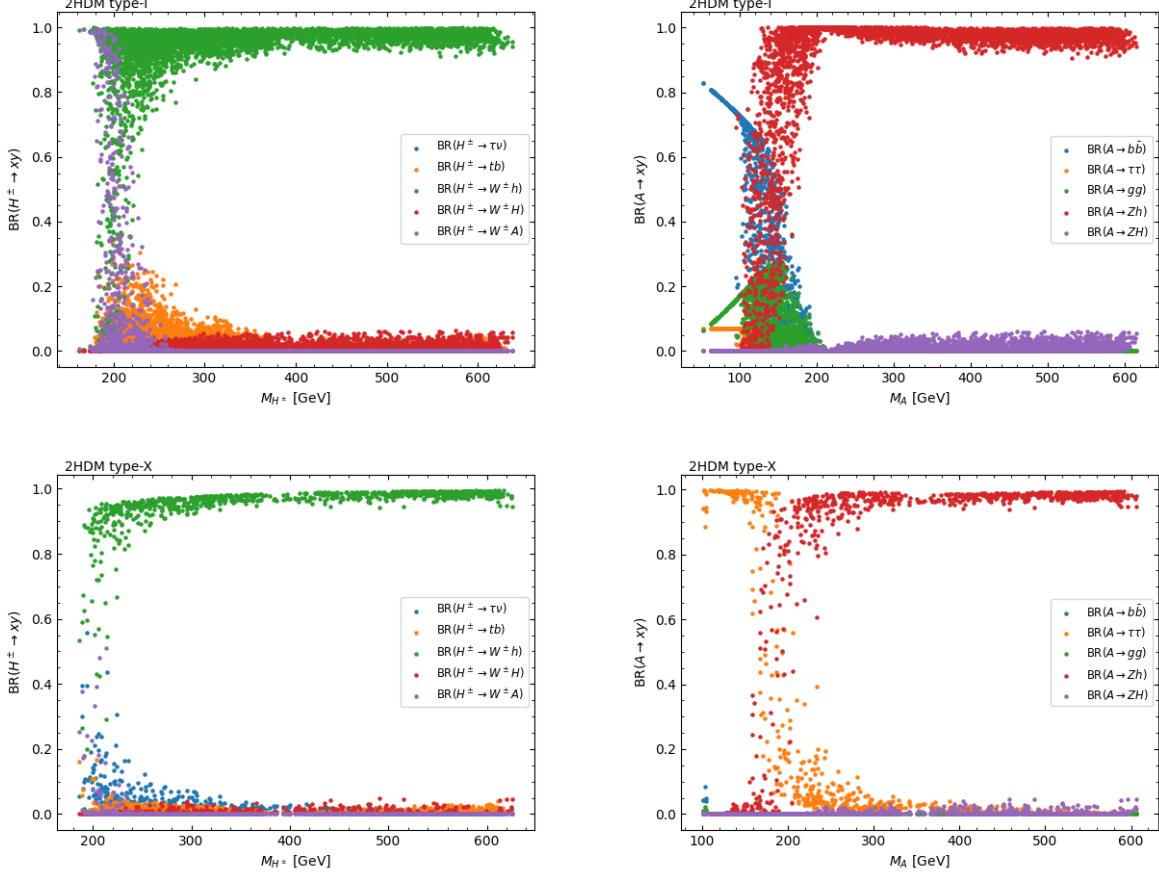


Figure 3: Branching ratios of the charged Higgs boson as a function of M_{H^\pm} (left) and CP-odd Higgs boson as a function of M_A (right). The upper panels are for 2HDM type I while the lower panels are for 2HDM type X.

is open it compete strongly with $H^\pm \rightarrow W^\pm h$ because the coupling $H^\pm W^\pm A$ is a pure gauge coupling while $H^\pm W^\pm h$ is suppressed by $\cos(\beta - \alpha)$. This is why we can see that, in some cases, the channel $H^\pm \rightarrow W^\pm A$ is the dominant one. The channel $H^\pm \rightarrow W^\pm H$ is negligible since it is suppressed by the parameter $\sin(\beta - \alpha)$ which is small in our scenario. Note that in 2HDM type I, charged Higgs coupling to fermions is proportional to $1/\tan\beta$ which makes $H^\pm \rightarrow tb, \tau\nu$ channels rather suppressed. We stress here that the dominance of the bosonic channels has been discussed previously in [60–64].

In Figure 3 (upper right panel) we depict the branching ratios of A as a function of M_A . It is clearly visible that before Zh threshold, the pseudo-scalar boson A decays dominantly into a pair of bottom quarks followed by $A \rightarrow gg$ and $A \rightarrow \tau\tau$ decays. The loop decay $A \rightarrow \gamma\gamma$ is suppressed by $1/\tan^2\beta$ and is smaller than 10^{-3} . Once we cross Zh threshold, the decay channel $A \rightarrow Zh$ becomes the dominant one when $M_A > M_Z + M_h$ since the coupling AZh is proportional to $\cos(\beta - \alpha)$ which is close to unity in our scenario. The channel $A \rightarrow ZH$ is suppressed by $\sin(\beta - \alpha)$ being close to vanish. Note that $A \rightarrow H^\pm W^\mp$ mode is kinematically not open after taking into account the M_W CDF measurement since $M_A < M_{H^\pm}$. This is, indeed, a strong effect of the new CDF measurement which closes the possibility to probe the charged Higgs boson via $A \rightarrow H^\pm W^\mp$ and/or $H \rightarrow H^\pm W^\mp$ decay channels.

Note that in the case of 2HDM type X as illustrated in Figure 3 (lower panels), we found that the charged Higgs decay dominantly to W^+h once W^+h threshold is crossed. Before W^+h threshold, there is a strong competition between $\tau\nu$, W^+h and W^+A channels, see Figure 3 (lower and upper left panels). Similarly for the decay of the CP-odd Higgs. Before the opening of $A \rightarrow Zh$, the channel $A \rightarrow \tau\tau$ is the dominant one and gets suppressed once $A \rightarrow Zh$ is open, see Figure 3 (lower right panel).

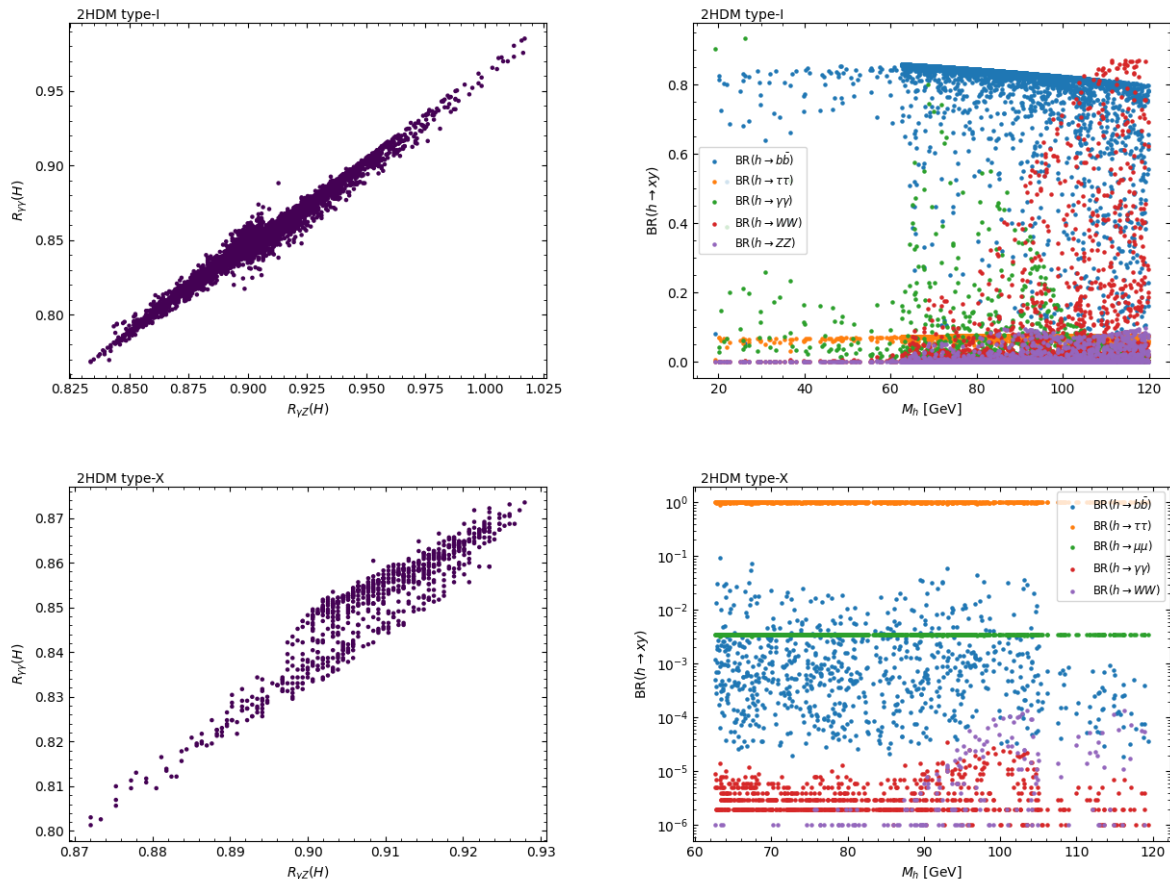


Figure 4: Left: Correlation between $R_{\gamma\gamma}(H)$ and $R_{\gamma Z}(H)$ for the SM-like Higgs. Right: Branching fractions for the light CP even. The plots are for 2HDM type I (upper panels) and type X (lower panels).

Before we end this section, we illustrate in Figure 4 (left upper and lower panels) the correlation between $R_{\gamma\gamma}(H) = \text{BR}(H \rightarrow \gamma\gamma)/\text{BR}(H \rightarrow \gamma\gamma)_{\text{SM}}$ and $R_{\gamma Z}(H) = \text{BR}(H \rightarrow \gamma Z)/\text{BR}(H \rightarrow \gamma Z)_{\text{SM}}$ for the SM-like Higgs both in 2HDM type I and type X. It is clear that $R_{\gamma Z}(H)$ is all time in the range $[0.85, 1]$ while $R_{\gamma\gamma}(H) \in [0.77, 0.97]$. One can see that they are linearly correlated with $R_{\gamma Z}(H)$ slightly larger than $R_{\gamma\gamma}(H)$ both in 2HDM type I and type X. However, in 2HDM type X, the ranges of $R_{\gamma\gamma}(H)$ and $R_{\gamma Z}(H)$ are a bit smaller compared to 2HDM type I. In Figure 4 (upper right panel) we illustrate the branching fractions of the light CP-even h in 2HDM type I. One can read that before the WW^* threshold, the dominant decay of h is into a pair of bottom followed by $h \rightarrow \gamma\gamma$ which could reach 90% close to the fermiophobic limit. In 2HDM type X as illustrated in Figure 4 (lower right panel), the decay $h \rightarrow \tau\tau$ is the dominant decay channel with a branching ratio almost above 99%. One can also read that $\text{BR}(h \rightarrow b\bar{b})$ does not exceed 10% and

$\text{BR}(h \rightarrow \mu^+ \mu^-)$ becomes of the order 3×10^{-3} .

It is also clear from Figure 4 that in 2HDM type I one can have the CP-even h as light as 20 GeV while in 2HDM type X we have $m_h > 63$ GeV.

4 Conclusion

Recently, CDF release its new measurement for W boson mass with unprecedented accuracy. The new CDF measurement presents a deviation from the SM prediction with a significance of 7.0σ . We have shown that in 2HDM with an inverted hierarchy, it is possible to solve the tension between the new CDF M_W measurement and the SM prediction. We found that to comply with the CDF measurement we need a positive T and this is possible in the case where $M_{H^\pm} > M_h, M_H, M_A$. The case of $M_{H^\pm} < M_h, M_H, M_A$ fail to reproduce the correct M_W measurement. Note also that the new CDF measurement for M_W push the charged Higgs to be larger than about 161 GeV. It is also found that the degenerate case $M_{H^\pm} = M_A$ which leads to a very small T parameter being excluded. We have presented a phenomenology of charged Higgs, CP-odd and the light CP-even higgses by illustrating their branching fractions both in 2HDM type I and type X. In the case of charged Higgs, we observe that the bosonic decay $H^\pm \rightarrow W^\pm h$ is the dominant one both for 2HDM type I and type X. While for the case of CP-odd, we have noticed that $A \rightarrow Zh$, once open, is the dominant mode both for 2HDM type I and X. However, before Zh threshold, $A \rightarrow b\bar{b}$ is the dominant mode for 2HDM type I while $A \rightarrow \tau\tau$ would dominate in the case of 2HDM type X. We have shown also that in this scenario and within 2HDM type X, $\text{BR}(h \rightarrow \mu^+ \mu^-)$ could be of the order 3×10^{-3} .

Note Added: While we were finishing this work, we received a paper [20] dealing with similar 2HDM study both in normal and inverted hierarchy. In the case of inverted hierarchy our results are in good agreement.

Acknowledgements: This work is supported by the Moroccan Ministry of Higher Education and Scientific Research MESRSFC and CNRST: Projet PPR/2015/6.

References

- [1] T. Aaltonen *et al.* (CDF collaboration), *Science* **376**, 170-176 (2022).
- [2] T. Aaltonen *et al.* [CDF], [arXiv:2110.14878 [hep-ex]].
- [3] P. A. Zyla *et al.* [Particle Data Group], *PTEP* **2020** (2020) no.8, 083C01.
- [4] M. Awramik, M. Czakon, A. Freitas and G. Weiglein, *Phys. Rev. D* **69** (2004), 053006 [arXiv:hep-ph/0311148 [hep-ph]].
- [5] M. E. Peskin and T. Takeuchi, *Phys. Rev. Lett.* **65** (1990), 964-967.
- [6] M. E. Peskin and T. Takeuchi, *Phys. Rev. D* **46** (1992), 381-409.
- [7] C. T. Lu, L. Wu, Y. Wu and B. Zhu, [arXiv:2204.03796 [hep-ph]].
- [8] A. Broggio, E. J. Chun, M. Passera, K. M. Patel and S. K. Vempati, *JHEP* **11** (2014), 058 [arXiv:1409.3199 [hep-ph]].
- [9] Y. Z. Fan, T. P. Tang, Y. L. S. Tsai and L. Wu, [arXiv:2204.03693 [hep-ph]].
- [10] H. Song, W. Su and M. Zhang, [arXiv:2204.05085 [hep-ph]].
- [11] H. Bahl, J. Braathen and G. Weiglein, [arXiv:2204.05269 [hep-ph]].
- [12] K. S. Babu, S. Jana and V. P. K., [arXiv:2204.05303 [hep-ph]].
- [13] T. Biekötter, S. Heinemeyer and G. Weiglein, [arXiv:2204.05975 [hep-ph]].
- [14] X. F. Han, F. Wang, L. Wang, J. M. Yang and Y. Zhang, [arXiv:2204.06505 [hep-ph]].
- [15] Y. Heo, D. W. Jung and J. S. Lee, [arXiv:2204.05728 [hep-ph]].
- [16] Y. H. Ahn, S. K. Kang and R. Ramos, [arXiv:2204.06485 [hep-ph]].
- [17] R. Benbrik, M. Boukidi and B. Manaut, [arXiv:2204.11755 [hep-ph]].
- [18] G. Arcadi and A. Djouadi, [arXiv:2204.08406 [hep-ph]].
- [19] K. Ghorbani and P. Ghorbani, [arXiv:2204.09001 [hep-ph]].
- [20] S. Lee, K. Cheung, J. Kim, C. T. Lu and J. Song, [arXiv:2204.10338 [hep-ph]].
- [21] X. K. Du, Z. Li, F. Wang and Y. K. Zhang, [arXiv:2204.05760 [hep-ph]].
- [22] A. Ghoshal, N. Okada, S. Okada, D. Raut, Q. Shafi and A. Thapa, [arXiv:2204.07138 [hep-ph]].
- [23] S. Kanemura and K. Yagyu, [arXiv:2204.07511 [hep-ph]].
- [24] A. Addazi, A. Marciano, A. P. Morais, R. Pasechnik and H. Yang, [arXiv:2204.10315 [hep-ph]].
- [25] J. M. Yang and Y. Zhang, [arXiv:2204.04202 [hep-ph]].
- [26] A. Strumia, [arXiv:2204.04191 [hep-ph]].
- [27] K. Sakurai, F. Takahashi and W. Yin, [arXiv:2204.04770 [hep-ph]].
- [28] X. Liu, S. Y. Guo, B. Zhu and Y. Li, [arXiv:2204.04834 [hep-ph]].
- [29] L. Di Luzio, R. Gröber and P. Paradisi, [arXiv:2204.05284 [hep-ph]].
- [30] P. Asadi, C. Cesarotti, K. Fraser, S. Homiller and A. Parikh, [arXiv:2204.05283 [hep-ph]].
- [31] J. J. Heckman, [arXiv:2204.05302 [hep-ph]].
- [32] E. Bagnaschi, J. Ellis, M. Madigan, K. Mimasu, V. Sanz and T. You, [arXiv:2204.05260 [hep-ph]].
- [33] A. Paul and M. Valli, [arXiv:2204.05267 [hep-ph]].
- [34] R. Balkin, E. Madge, T. Menzo, G. Perez, Y. Soreq and J. Zupan, [arXiv:2204.05992 [hep-ph]].
- [35] M. Endo and S. Mishima, [arXiv:2204.05965 [hep-ph]].
- [36] M. D. Zheng, F. Z. Chen and H. H. Zhang, [arXiv:2204.06541 [hep-ph]].
- [37] L. M. Carpenter, T. Murphy and M. J. Smylie, [arXiv:2204.08546 [hep-ph]].
- [38] O. Popov and R. Srivastava, [arXiv:2204.08568 [hep-ph]].
- [39] T. A. Chowdhury, J. Heeck, S. Saad and A. Thapa, [arXiv:2204.08390 [hep-ph]].
- [40] V. Cirigliano, W. Dekens, J. de Vries, E. Mereghetti and T. Tong, [arXiv:2204.08440 [hep-ph]].
- [41] A. Bhaskar, A. A. Madathil, T. Mandal and S. Mitra, [arXiv:2204.09031 [hep-ph]].

- [42] S. Baek, [arXiv:2204.09585 [hep-ph]].
- [43] J. Cao, L. Meng, L. Shang, S. Wang and B. Yang, [arXiv:2204.09477 [hep-ph]].
- [44] J. Kawamura, S. Okawa and Y. Omura, [arXiv:2204.07022 [hep-ph]].
- [45] K. I. Nagao, T. Nomura and H. Okada, [arXiv:2204.07411 [hep-ph]].
- [46] K. Y. Zhang and W. Z. Feng, [arXiv:2204.08067 [hep-ph]].
- [47] D. Borah, S. Mahapatra and N. Sahu, [arXiv:2204.09671 [hep-ph]].
- [48] Y. Cheng, X. G. He, F. Huang, J. Sun and Z. P. Xing, [arXiv:2204.10156 [hep-ph]].
- [49] A. Batra, S. K. A, S. Mandal and R. Srivastava, [arXiv:2204.09376 [hep-ph]].
- [50] G. C. Branco, P. M. Ferreira, L. Lavoura, M. N. Rebelo, M. Sher and J. P. Silva, Phys. Rept. **516** (2012), 1-102 [arXiv:1106.0034 [hep-ph]].
- [51] S. L. Glashow and S. Weinberg, Phys. Rev. D **15** (1977), 1958
- [52] D. Eriksson, J. Rathsman and O. Stal, Comput. Phys. Commun. **181** (2010), 189-205 [arXiv:0902.0851 [hep-ph]].
- [53] G. Aad *et al.* [ATLAS and CMS], Phys. Rev. Lett. **114** (2015), 191803 [arXiv:1503.07589 [hep-ex]].
- [54] J. Haller, A. Hoecker, R. Kogler, K. Mönig, T. Peiffer and J. Stelzer, Eur. Phys. J. C **78** (2018) no.8, 675 [arXiv:1803.01853 [hep-ph]].
- [55] P. Bechtle, D. Dercks, S. Heinemeyer, T. Klingl, T. Stefaniak, G. Weiglein and J. Wittbrodt, Eur. Phys. J. C **80** (2020) no.12, 1211 [arXiv:2006.06007 [hep-ph]].
- [56] P. Bechtle, S. Heinemeyer, T. Klingl, T. Stefaniak, G. Weiglein and J. Wittbrodt, Eur. Phys. J. C **81** (2021) no.2, 145 [arXiv:2012.09197 [hep-ph]].
- [57] F. Mahmoudi, Comput. Phys. Commun. **180** (2009), 1579-1613 [arXiv:0808.3144 [hep-ph]].
- [58] S. Schael *et al.* [ALEPH, DELPHI, L3, OPAL, SLD, LEP Electroweak Working Group, SLD Electroweak Group and SLD Heavy Flavour Group], Phys. Rept. **427** (2006), 257-454 [arXiv:hep-ex/0509008 [hep-ex]].
- [59] J. de Blas, M. Pierini, L. Reina and L. Silvestrini, [arXiv:2204.04204 [hep-ph]].
- [60] A. Arhrib, R. Benbrik and S. Moretti, Eur. Phys. J. C **77** (2017) no.9, 621 [arXiv:1607.02402 [hep-ph]].
- [61] H. Bahl, T. Stefaniak and J. Wittbrodt, JHEP **06** (2021), 183 [arXiv:2103.07484 [hep-ph]].
- [62] A. Arhrib, R. Benbrik, M. Krab, B. Manaut, S. Moretti, Y. Wang and Q. S. Yan, JHEP **10** (2021), 073 [arXiv:2106.13656 [hep-ph]].
- [63] Y. Wang, A. Arhrib, R. Benbrik, M. Krab, B. Manaut, S. Moretti and Q. S. Yan, JHEP **12** (2021), 021 [arXiv:2107.01451 [hep-ph]].
- [64] A. Arhrib, R. Benbrik, M. Krab, B. Manaut, S. Moretti, Y. Wang and Q. S. Yan, Symmetry **13** (2021) no.12, 2319 [arXiv:2110.04823 [hep-ph]].

Appendix A

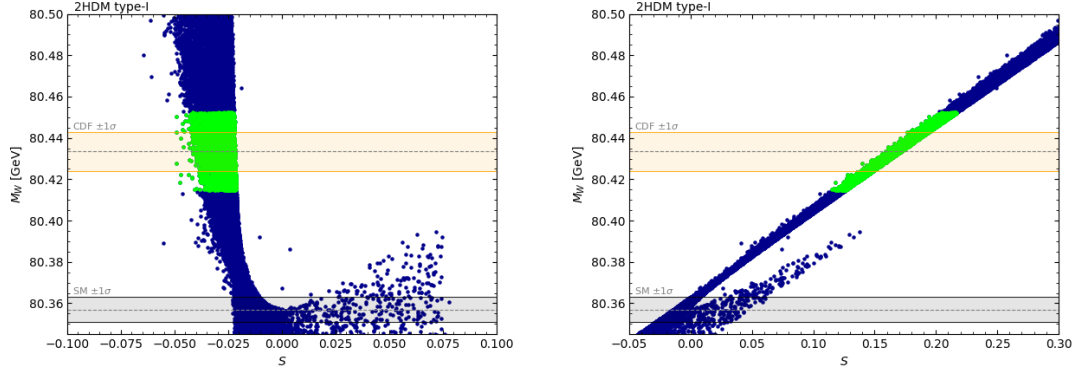


Figure A1: The 2HDM prediction for the W boson mass as a function of S (left panel) and T (right panel). The light green band represents points within the 2σ CDF M_W measurement.

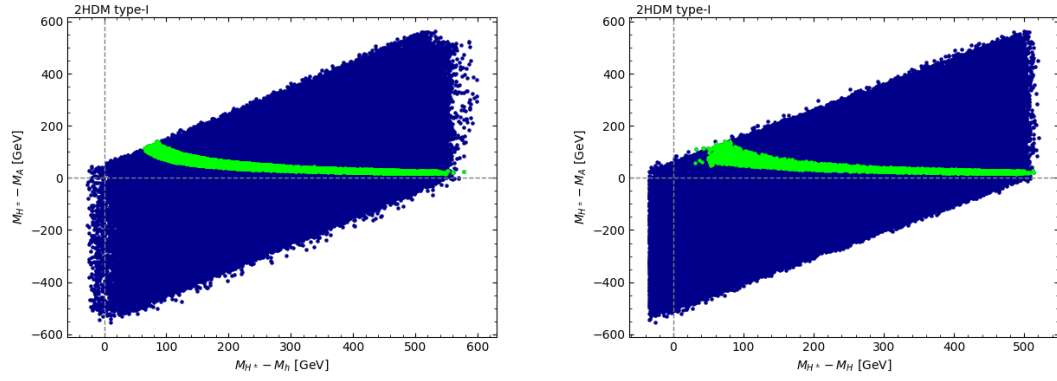


Figure A2: Points from the scan in the $(M_{H^\pm} - M_h, M_{H^\pm} - M_A)$ plane (left panel) and $(M_{H^\pm} - M_H, M_{H^\pm} - M_A)$ plane (right panel). The light green band represents points within the 2σ CDF M_W measurement.